A NEW TYPE OF QUALITATIVE CHANGE IN CHAOTIC DYNAMICS CAUSED BY RIDDLED BASINS

(Proceeding)

Satoshi Hayama

Rakuyo Technical High School, Kyoto, Japan

A new type of qualitative change in chaotic dynamics is discussed and illustrated. In this case, as the control parameter is varied, the destruction of the chaotic attractor occurs quite secretly, and the average lifetime of chaotic transients decreases extremely slowly. Furthermore, in the course of this decrease, periodic attractors appear many times. Such a change can be observed in some non invertible maps which have attractors in a bounded area, and have, in the boundary of this area, a coexisting chaotic attractor whose basin is riddled. It is shown by numerical considerations that such a change may result from the invasion of pieces of the riddled basin of the coexisting chaotic attractor into the chaotic object in the bounded area.

1. Introduction

Recent work by J.C.Alexander et al.[1] has shown that there can exist chaotic systems having attractors for which at any point in its basin of attraction an open ball with an arbitrarily small radius always contains pieces of another attractor basin. In such a case the basin is called [1,2] "riddled basin". Several theoretical and experimental works which support these findings have appeared [3-11]. This behavior can arise in systems that possess chaotic dynamics in a smooth invariant manifold of lower dimension than that of the full phase space.

In this work such systems having an attractor B (or, attractors B_1, B_2,$\cdots$,B_n) in a bounded area (namely, a closed area in which trajectries are confined) and a coexisting chaotic attractor A whose basin is riddled are studied. Following prey-predator model [12] is one of such systems;

$$\begin{aligned} x_{n+1} &= a x_n (1 - x_n - y_n) \\ y_{n+1} &= b y_n (1 + c x_n) . \end{aligned} \qquad n = 1, 2, 3, \cdots \qquad (1)$$

The system (1) is one of the simple two-dimensional noninvertible maps. In this map, the x-axis is an invariant manifold of the system. The dynamics on this manifold is the well known logistic map which has chaotic attractor A as the parameter a is suitably chosen in $3.699\cdots < a \leqq 4$. Each orbit starting from inside of the area D which is bounded by lines $x = 0$, $y = 0$, and $1 - x - y = 0$ is confined as parameter a, b, c are suitably chosen. In the following argument, parameter a, c are fixed suitably (typically 4, 5 respectively), and parameter b is treated as a control parameter.

How the bifurcation of the attractor B goes on when the parameter b, which control the stability of the attractor A perpendicular to the x-axis, is varied? An answer to this problem is given by the numerical considerations for the system (1), with finding a

Let F be a C^2 planar map for which the x-axis is invariant. Suppose that F has an attractor A which supports an invariant measure μ in the x-axis. Writing F with its components as

$$F(x,y) = (f(x,y),\ g(x,y)), \tag{2}$$

and n-iterates as

$$F^{(n)}(x,y) = (f^{(n)}(x,y),\ g^{(n)}(x,y)). \tag{3}$$

For the system (1), components of F are given as

$$\begin{aligned} f(x,y) &= ax(1-x-y) \\ g(x,y) &= by(1+cx). \end{aligned} \tag{4}$$

For each point of $(x,0) \in A$ the normal Lyapunov exponent $L_\perp(x)$ is defined by

$$L_\perp(x) = \lim_{n\to\infty} \frac{1}{n} \ln [D_y g^{(n)}](x,0). \tag{5}$$

It has been shown by J.C.Alexande et al.[1] that $L_\perp(x)$ exist and is independent for almost all x with respect to μ, and that if this typical value $L_\perp$ is negative then most points near A in R^2 are attracted to A. For the system (1) $L_\perp$ (which is controlled by the parameter b, so is represented as L(b), too) is given by

$$L_\perp = L(b) = \lim_{n\to\infty} \frac{1}{n} \sum_{i=1}^{n} \ln \{b(1+cx_i)\}, \qquad x_i = f^{(i)}(x,0). \tag{6}$$

Regarding b_c as the critical point of b at which L(b) changes in its sign, it is shown in the following numerical and theoretical arguments that, when $L_\perp$ changes from its positive value to negative value at $b = b_c$, the attractor A changes in its stability in y space from a simple reppler to an attractor which has a riddled basin. Moreover the following aspects will become apparent numerically.

(1) As the parameter b has decreased from b_c, after the periodic attractor B developed into a chaotic object this chaotic attractor B changes promptly to the chaotic quasi attractor (namely, chaotic transient whose average lifetime is very long).

(2) But this change begins quite secretly in contrast to the crises [13] in which sudden destructions of chaotic attractors occur.

(3) The average lifetime of this quasi attractor decreases very slowly as the parameter b is varied. The width of the parameter range, from the point at which the destruction of chaotic attractor has already begun, to the point at which the average lifetime becomes about 10^4, reaches about 1/2 times the width of the parameter range, from the point at which the period doubling bifurcation begins, to the point at which this bifurcation reaches ∞ period. Therefor, chaotic orbits can be observed in enouph iterates in the quite wide range of the parameter. In this meaning, too, it is suitable to call this chaotic transient chaotic "quasi attractor".

(4) In the course of decreasing of the average lifetime, periodic attractors appear in many times.

2. Riddled Basin, chaotic quasi attractor

The system (1) has the following two fixed points which are important to the following argument in addition to the self evident fixed point (0, 0):

$$p_A = (1-1/a,\ 0),$$
$$p_B = (-1/c+1/bc,\ 1-1/a+1/c-1/bc)\ . \tag{7}$$

The bifurcation of the problem occurs in the parameter area R_5 in Fig.1 [12]. Period doubling bifurcation of the fixed point p_B which exists in the bounded area D starts when the parameter b decreases from the upper side of the boundary of R_5. Fig.2 is a bifurcation diagram in this case, in which multiple initial conditions are chosen, setting the parameter a, c as 4, 5 respectively and varying the parameter b from 0.261 to 0.251. It will be recognized in Fig.2 that the chaotic object appears after the period doubling bifurcation reached ∞ period at $b \fallingdotseq 0.255927$, and that the chaotic object changes promptly to the chaotic transient. Backgrounds in Fig.2 represent points in the attractor A which exists on the unit interval $I=[0, 1]$ in the x-axis, and this shows that there exist initial points from which orbits leave soon for the attractor A within 10^4 iterates

Black part in Fig.3(a) shows the basin of 16-periodic attractor B, which lies about 0.1 in y space as $b=0.256$, while white part shows the basin of attractor A. Fig.3(b), where the fixed point p_B is placed in the center, is an enlargement of a part of Fig.3(a). Fig.3(c) is a stretched figure of Fig.3(a) for $0 \leqq y \leqq 0.05$. It seems from these figures that the basin of attractor A is riddled. But the basin of attractor B is partially riddled because there are some neighborhoods in which each points is attracted to the periodic points. Moreover it is conjectured in Fig.3(b) that there will exist an invariant manifold to which layers of two basins are accumulating alternately.

In Fig.4, the smooth curve which links the fixed point p_B and the fixed point p_A is a stable manifold (M_1) of p_B, and also, is an unstable manifold of p_A. Two smooth curves which depart out of p_B on either side and head for the two-periodic points in x-axis are an unstable manifold (M_2) of p_B. But when an orbit leaves from p_B along by the manifold M_2, this orbit begins to separate from the manifold M_2 at some position (from which the manifold is drawn by the dotted lines) and makes amplitude of vibration larger to either side of manifold M_2.

Small circles in Fig.5 show the distribution ratio (d_B) of points of the basin of attractor B over the interval [0.7, 0.8] of x for the range $0.0005 < y < 0.01$. In this case, from the data used in Fig.5 the following power law is recognized numerically:

$$d_B \fallingdotseq 26800 \times y^{2.81}\ . \tag{8-1}$$

But both of the coefficient and the exponent in (8-1) take different values when another interval of x or another range of y is taken. For the full range of x in D the ratio d_B is calculated as

$$d_B \fallingdotseq 3100 \times y^{2.75}. \tag{8-2}$$

Supposing d_B, modelling after (8-1,2), to be the following form

$$d_B(y)=\alpha y^{\gamma}, \tag{9}$$

the value of the exponent γ in (9) for the neighborhood of p_A can be estimated theoretically (in the full paper, to be about 3.55 for $b=0.256$).

Fig.6 shows an object of a chaotic quasi attractor of the system (1) calculated for the initial condition (0.2, 0.2) for $b=0.255$. This orbit continues about 99350 iterates until it becomes $y<10^{-6}$, while as shown in Fig.7 this orbit becomes $y<10^{-6}$ in only 50 iterates after it began to leave for $y=0$. In other words, the orbit keeps $y>0.04$ in 99300 iterates and pictures an object shown in Fig.6. In the upper figure of Fig.7, 1000 iterates of y of this orbit are plotted in the vertical after initial 98500 iterates, and the lower figure displays the same steps in $\log(y)$. In Fig.6, a small circle shows the fixed point p_B, and points which heads under either side near p_B go along by the unstable manifold M_2 of p_B. This manifold penetrates the chaotic object and reaches to the 2-periodic points in the x-axis. As shown in Fig.7 the orbit is highly blown up before beginning to leave for $y=0$. This behavior occurs for the orbit which is blown up along by the manifold M_1 after it fell in near M_1. The orbit chooses either to trace in the chaotic object again or to leave for the attractor A after coming back again into the chaotic object.

3. Secret destruction of the chaotic attractor

In Fig.8, the white part shows a set of initial points from which orbits become $y<10^{-6}$ within initial 10^3 iterates, while the black part is the complement set. The orbit from each point in this black part pictures much the same figure as Fig.6, though the lifetime depends on each initial point. Therefor, let us call the set of the black points 'quasi basin' of the chaotic quasi attractor here. But the set of points of the quasi basin depends on the number of initial iterates, computing precision, and parameters too. In any case, the figure of the quasi basin becomes transparent as the number of initial iterates is increased. Fig.9 shows the aspect of lifetimes which were calculated for 500 initial conditions uniformly chosen in the segment $0.2\leqq x\leqq 0.25$, $y=0.2$, which lies in the area filled sufficiently by points of the quasi basin of the chaotic quasi attractor B. Fig.10 shows a numerical result for the surviving number N of chaotic orbits as the function of t (the number of iterates), where data from 1.2×10^4 initial conditions uniformly chosen in the same segment as in Fig.9 was used. This figure predicts the following exponential decay form for N;

$$N=N_0\exp(-t/\tau), \tag{10}$$

where N_0 is the number of initial conditions, and τ is the average lifetime of chaotic transients. In this case, τ is calculated about 1.04×10^5. This is the same form as the case of the crisis [13] in the Hénon map. The formula (10) permits us thinking the system has the statistical nature that each orbit of chaotic transient falls, with probability $1/\tau$ per one-iterate, into the "pitfall" from which the orbit leaves for $y=0$. That

is, pitfalls are distributed on virtual support μ of the chaotic quasi attractor with average density $1/\tau$, represented as μ_d:

$$\mu_d = 1/\tau . \tag{11}$$

Let us consider the parameter dependence of μ_d, supposing the following power law,

$$\mu_d = \alpha (b_d - b)^{\kappa}, \tag{12}$$

where b_d is the critical point of the parameter b, at which the chaotic attractor B changes to the chaotic transient. Fig.11 shows a numerical result of the parameter dependence of the average lifetime τ, calculated setting b_d as 0.2558018, where collapse of a chaotic orbit canbe observed already. Each point In Fig.11 was obtained by using data from 500 initial conditions uniformly chosen in the same segment as in Fig.9 for each of 26 values of b in the range 0.2532~0.2557. The solid line in Fig.11 was fitted to the points. In this case, the value of κ is estimated to be about 1.30. But, when b_d increases to a little, κ increases sensitively. For example, as $b_d = 0.2558115$, κ becomes about 1.33. At this value of b the same chaotic object as Fig.6 can be observed only for quite many iterates (about 10^7 or more) as shown in Fig.12, though the finding of the collapse of the chaotic object has never been succeeded. But it can be thought that the destruction of the chaotic attractor has occurred already in this level of b because the orbit should have chances to go into near the manifold M_1, or M_2, though rarely and intermittently. In any case, it is clear numerically that the absolute value of the exponent κ is larger than 1. Then, the parameter dependence of μ_d is like the curve (a) in Fig.13, and the invasion of the pitfalls begins secretly as if cusps with the pitfalls invade. On the other hand, in case of the boundary crises, which occur for chaotic attractors in one-dimensional quadratic maps, two-dimensional invertible maps and so on, the type of like the curve (b) in Fig.13 can occur because the value of κ is 1/2 or more ($\kappa > 1$ occur in case of weakly dissipative two-dimensional invertible maps), and changes in those chaotic dynamics are sudden as has been shown by C.Grebogi et al [13].

To summarize, the occurrence of this secret destruction is due to the following two dynamical caracteristics. The one is that the cobweb of pitfalls from which orbits leave for the attractor A is already prepared in the area which growing chaotic orbits will occupy. As for the other, in the beginning of destruction chaotic orbits get to adventure rarely and intermittently out of the territory on four small secure islands into the wide area in which the cobweb of pitfalls exists.

4. Longlife aspect in chaotic quasi attractors

The second characteristic of this quasi attractor is that the average lifetime decreases very slowly as the parameter b is varied. The width of the parameter range, from the point $b = 0.2558018$, at which the destruction of the chaotic attractor has already begun, to thepoint $b = 0.2537$, at which the average lifetime becomes about 10^4, reaches about 0.44 times the width 4.73×10^{-3} of the parameter range, from the point $b = 0.260655$, at which period doubling bifurcation begins, to the point at which this bifurcation reaches ∞ period. Moreover, the 3rd characteristic is that periodic

attractors appear many times in the course of decreasing of average lifetime τ. Fig.14 shows the parameter dependence of the average lifetime of chaotic transients obtained numerically using data from 100 initial conditions in the same segment as in Fig.9 for each value of b in the range 0.246～0.256. Diverging aspects in Fig.14 indicates the existence of periodic attractors, 10-periodic attractor for (a), 6-periodic attractor for (b). And also, other periodic attractors, which do not appear in this graph, can be found. For example, 36-periodic attractor appears around $b = 0.2557$. It can be thought that the reason why periodic attractors apear many times is that the bifurcation of this case may occur similar to that of logistic map, because, as the parameter b decreases, the position of the orbit becomes lower in y space, then the range of x in which orbits visit proceeds to spread near to the range of attractor A.

5. Conclusion

Some systems which have the following characteristics exist. In case that the basin of the chaotic attractor A which exists on a part of the boundary of the bounded area D becomes riddling when the normal Lyapunov exponent $L_\perp$ on A changes to negative in its sign by varying the control parameter, there exist such an attractor B in D that the characteristics of the bifurcation of the attractor B by varying the same control parameter is as follows.

(1) After the periodic attractor B bifurcated to the chaotic attractor, the destruction of the chaotic attractor begins promptly by the invasion of pieces of the riddled basin of A into the chaotic object B.

(2) The destruction of the chaotic attractor B begins quite secretly.

(3) the average lifetime of the chaotic transients decreases extremely slowly as the control parameter is varied.

(4) In the course of this decreasing, periodic attractors appear many times over.

References

[1]J.C.Alexander, J.A.Yorke, Z.You, and I.Kan, Int.J.Bif.Chaos 2 (1992) 795.
[2]J.C.Sommerer, and E.Ott, Nature 365 (1993) 136.
[3]E.Ott, J.C.Sommerer,J.C.Alexander, I.Kan, and J.A.York, Phys.Rev.Lett. 71, (1993) 41.
[4]E.Ott and J.C.Sommerer, Phys.Lett. A 188 (1994) 39.
[5]E.Ott, J.C.Alexander, I.Kan, J.C.Sommerer, and J.A.York, Physica 76D (1994) 384.
[6]I.Kan, Bull.Am.Math.Soc. 31 (1994) 68.
[7]P.Ashwin, J.Buescu, and I.Stewart, Phys.Lett. A 193 (1994) 126.
[8]R.H.Parmenter and L.Y.Yu, Phys.Lett. A 189 (1994) 181.
[9]J.F.Heagy, T.L.Carroll, and L.M.Pecora, Phys.Rev.Lett. 73 (1994) 3528.
[10]T.Kapitaniak, J.Phys. 28 (1995) L63.
[11]T.Kapitaniak, and L.O.Chua, Int.J.Bif.Chaos 6 (1996) 357
[12]S.Hayama, Seibutubuturi (japan) 109 (1980) 57.
[13]C.Grebogi,E.Ott,J.A.Yorke,Physica 7D (1983) 181

Fig.1

Parameter regions of different states for system (1). R_1; (0, 0)is stable, R2; p_A in (7) is stable, R_3; p_B in (7) is stable. (Reproduced from reference [12].)

Fig.2

Bifurcation diagram for the system (1) for $a=4$, $c=5$, in which multi initial conditions, (0.0001, 0.2), (0.1001, 0.2), (0.2001, 0.2), (0.3001, 0.2) are taken, and 50 iterates after initial 10^4 iterates are dotted for each value of b. The upper figure shows x component, while the lower one shows y component. Backgrounds in the upper one show points of orbits on the attractor A, which exists on the unit interval [0, 1] of x.

Fig.3

Basin of attraction of the system (1) for $a=4$, $b=0.256$, $c=5$. Black part shows the basin of 16-periodic attractor B, which lies about 0.1 height in y space in the bounded area D, while white part shows the basin of attractor A. Fig.(b) is an enlargement of some square region in Fig.(a), in Fig.(b) the fixed point p_B is placed on the center. Fig.(c) displays the stretched figure of the region $0 \leqq y \leqq 0.05$ in Fig.(a).

Fig.4

Stable, and unstable manifold of the fixed point p_B. Stable manifold M_1 links the fixed point p_B and the fixed point p_A which exist in the x-axis. Unstable manifold M_2 which depart out of p_B on either side and head for the two-periodic points in the x-axis.

Fig.5

Each small circle in this figure indicates the distribution ratio d_B of points of the basin of attractor B over the interval [0,7, 0.8] of x for each of 9 values of y in the range 0.01～0.0005. A straight line in this figure was fitted to the points by least-square method. In this case, power law $d_B \fallingdotseq 26800 \times y^{2.8}$ obeys numerically.

Fig.6

An object of a chaotic quasi attractor of the system (1) for $a=4$, $b=0.255$, $c=5$, calculated for the initial condition (0.2,0.2) in the precision of 72 digits below the decimal point. An small circle in this figure is the fixed point p_B. This orbit continues about 99350 iterates until it becomes $y<10^{-6}$, while the orbit becomes $y<10^{-6}$ in only 50 iterates after it began to leave for the attractor A.

Fig.7

The upper figure indicates 1000 iterates of y component of the same orbit as in Fig.6 after initial 98500 iterates. The lower one shows the same steps in log (y).

Fig.8

Quasi basin of chaotic quasi attractor B for the same other conditions as in Fig.6. White part corresponds to a set of initial points from which orbits become $y < 10^{-6}$ within initial 10^3 iterates, while black part is the complement set, namely a quasi basin, from each point of which an orbit are still surviving in 10^3 iterates.

Fig.9

A sketch of lifetimes calculated for 500 initial conditions on a segment $0.2 \leqq x \leqq 0.25$, $y = 0.2$ for the same other conditions as in Fig.6. These values of lifetime are hypersensitive to the small varying in the initial condition, parameters, and computing precision to some deep level.

Fig.10

Numerical results for surviving number N of chaotic orbits as a function of time t (the number of iterates). These results were obtained using data from initial 1.2×10^4 conditions uniformly chosen in the same segment as in Fig.9 for the same other conditions as in Fig.6. The vertical axis in this figure is represented on a logarithmic scale.

Fig.11

Parameter dependence of the average lifetime of chaotic transients. Each point was obtained numerically using data from 500 initial conditions uniformly chosen in the same segment as in Fig.9 for each of 26 values of parameter b in a range $0.2532 \sim 0.2557$, setting b_d as 0.2558018. A straight was fitted to the points, to obtain the parameter dependence of the average life τ. In this case, τ is proportional to $(b_d - b)^{-1.30}$

Fig.12

A chaotic orbit which adventure rarely and intermittently out of the territory on four small secure islands into the wide area in which the cobweb of pitfalls exists. Figure (a) shows initial 10^6 iterates followed by 2.5×10^5 iterates in Figure (b), 5×10^5 iterates in Figure (c), and 10^7 iterates in Figure (d). Calculation was done in the precision of 96 digits below the decimal point for $a = 4$, $b = 0.2558115$, $c = 5$, and initial condition (0.2, 0.2).

Fig.13

Schematic expression of two types of destructions of chaotic attractors. μ_d represents the average pitfall density in virtual support μ of chaotic quasi attractor. Type (a) shows the secret change, while type (b) shows the sudden change.

Fig.14

Average lifetime of chaotic transients obtained numerically using data from 100 initial conditions in the same segment as in Fig.9 for each value of b in the range $0.246 \sim 0.256$. Diverging aspects in the figure imply the existence of periodic attractors, 10-periodic attractor for (a), 6-periodic attractor for (b).

Fig.1

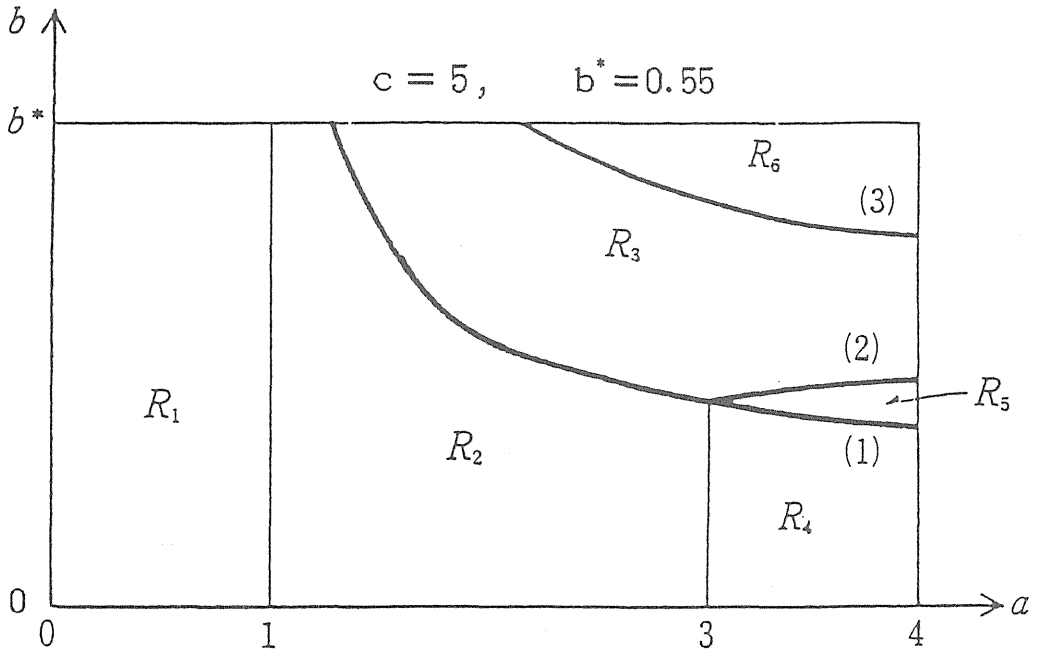

Fig.2

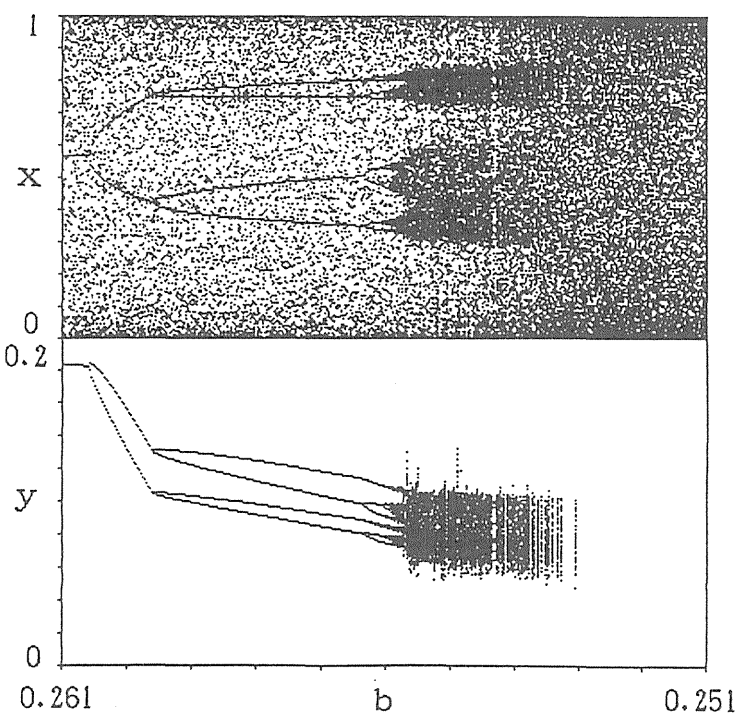

Fig.3

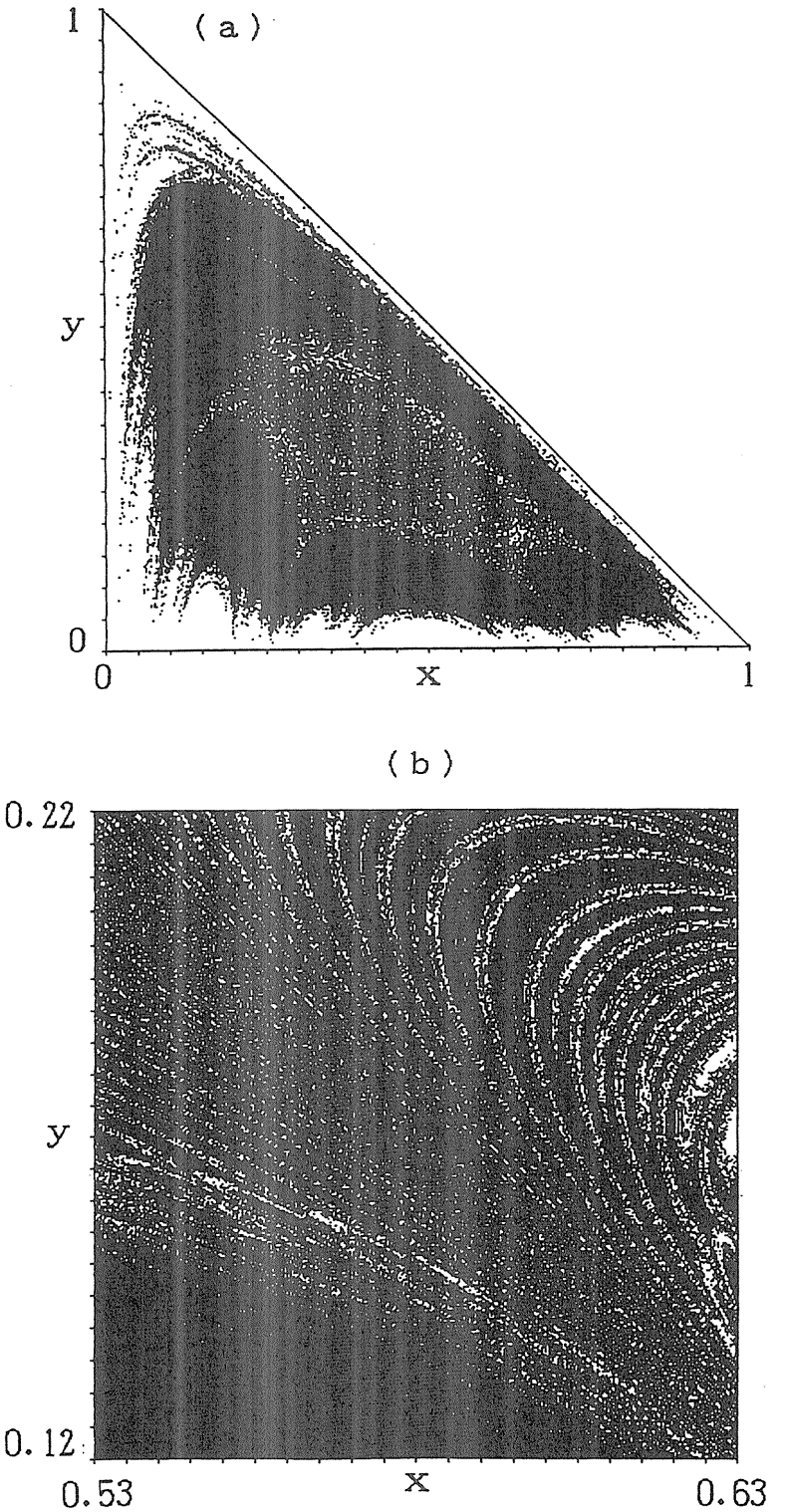

Fig.3

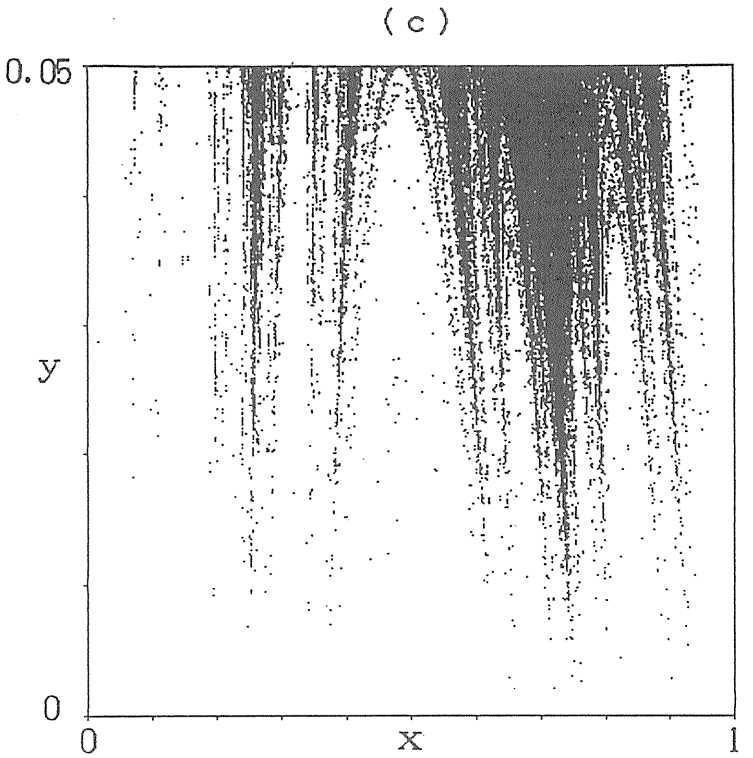

Fig.4

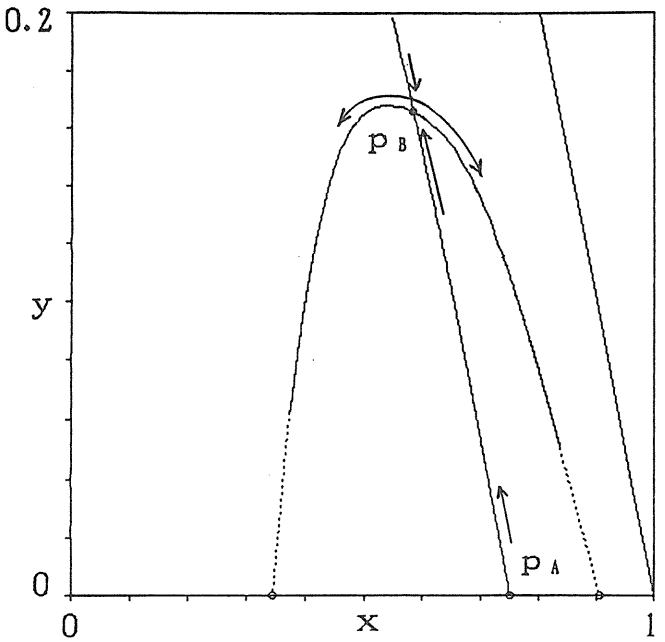

Fig.5

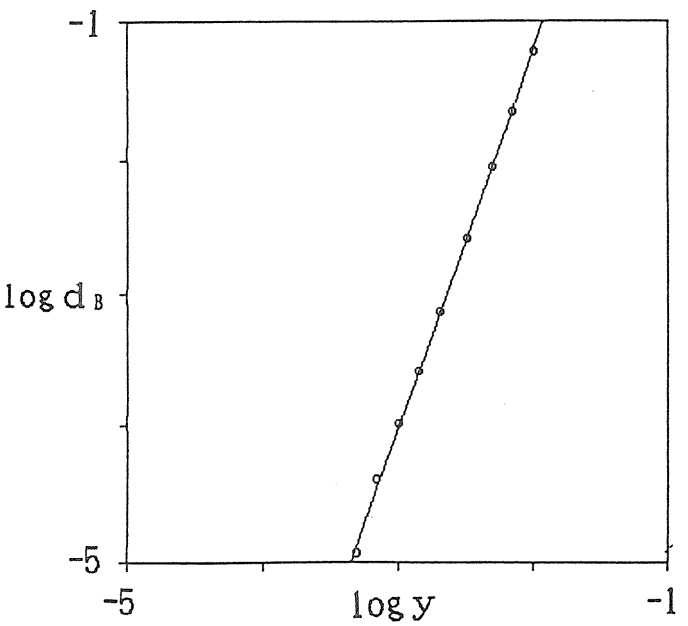

Fig.6

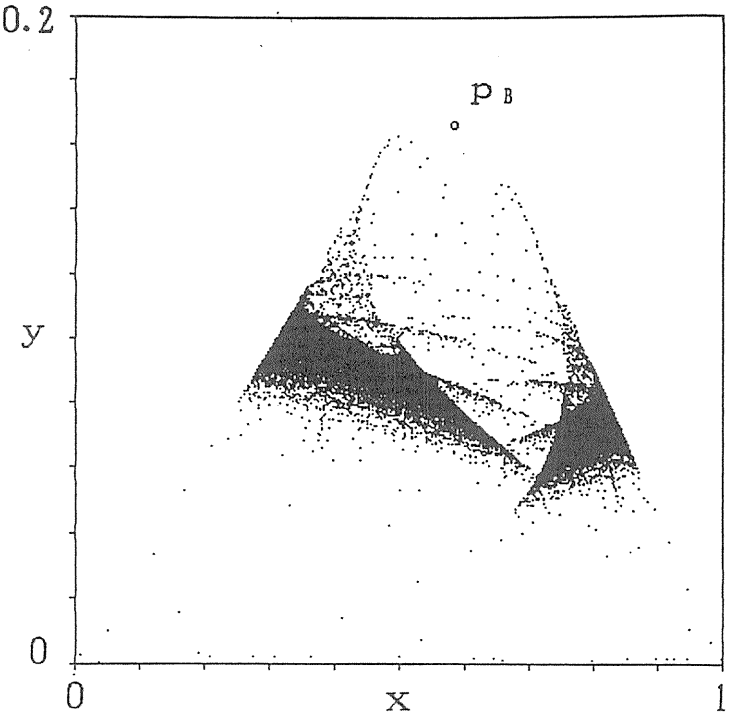

Fig.7

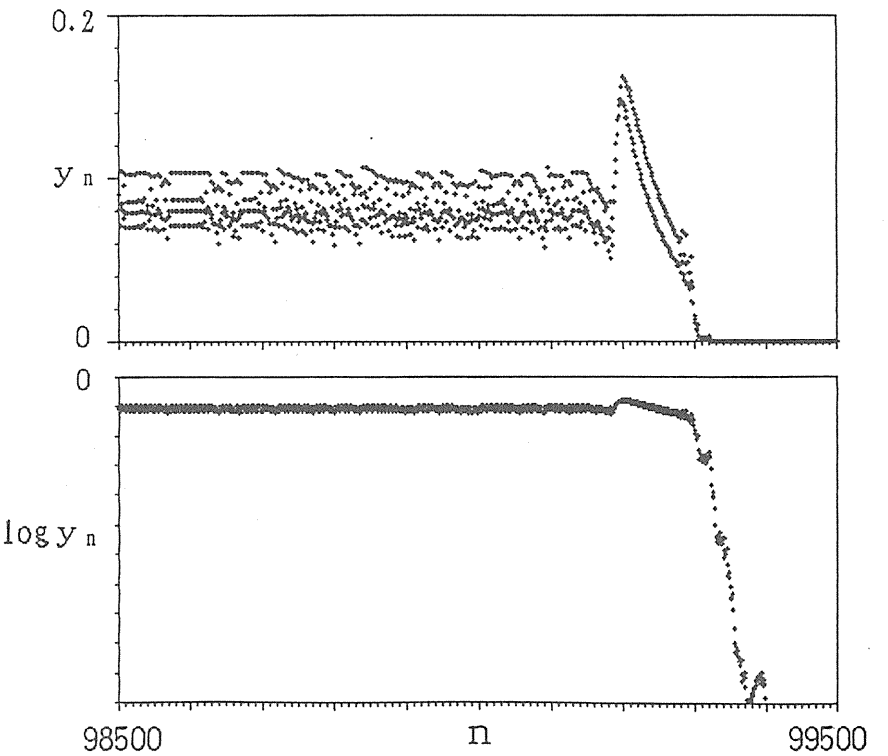

Fig.8

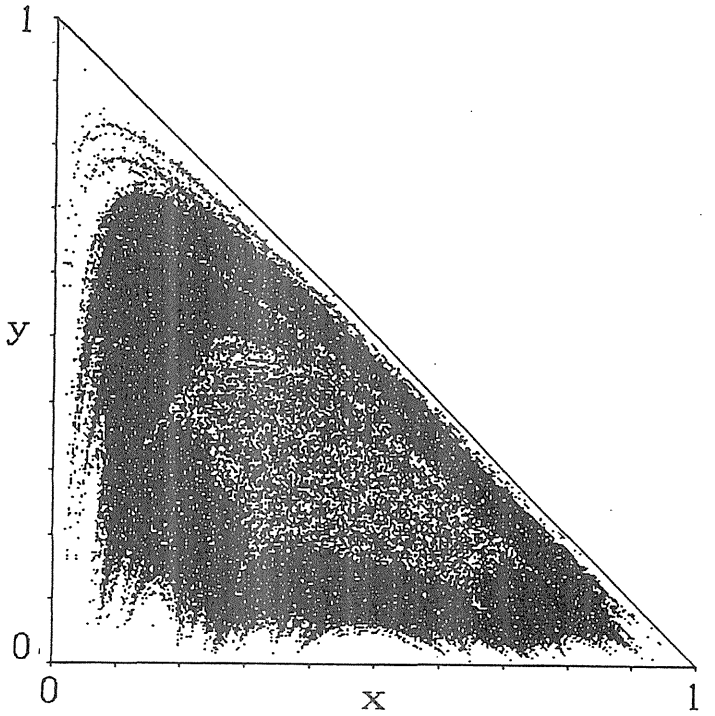

Fig.9

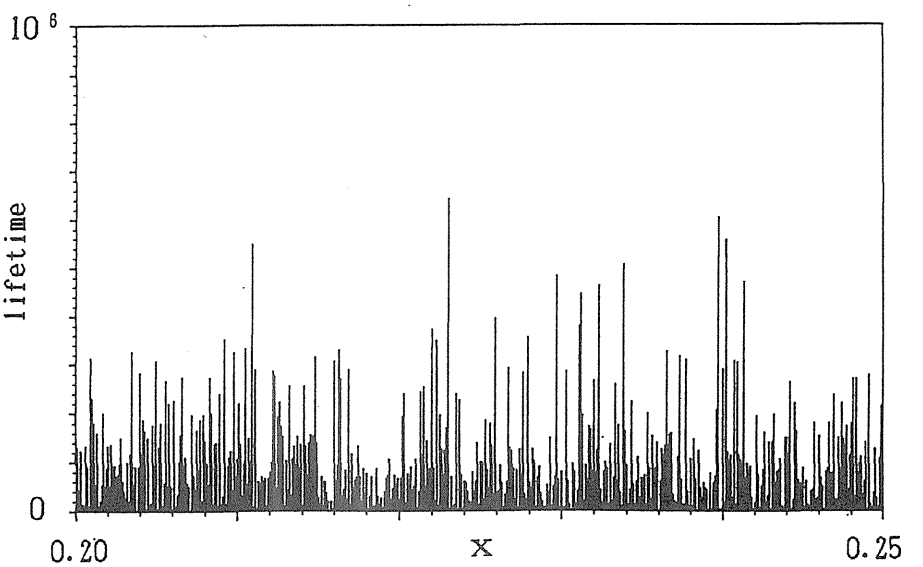

Fig.10

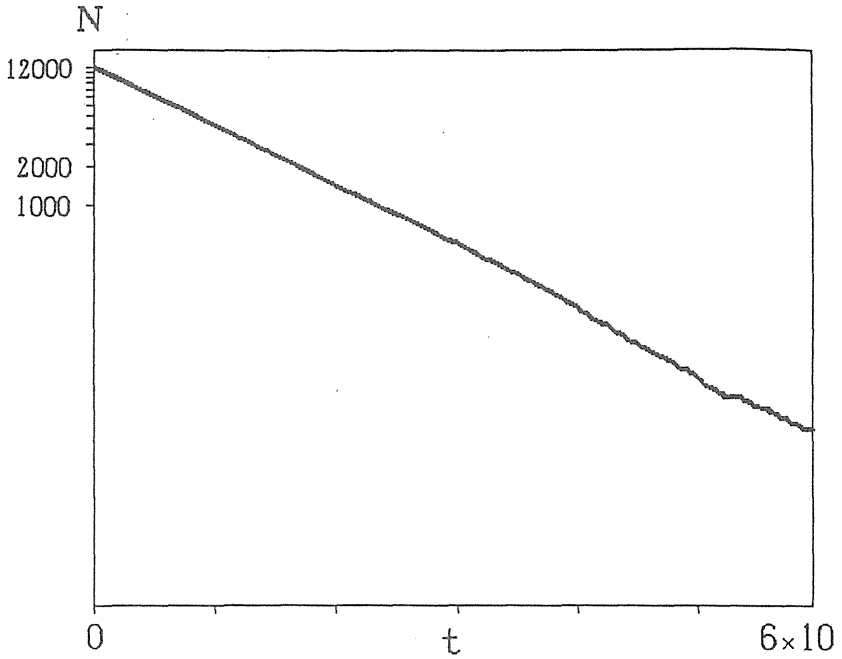

Fig.11

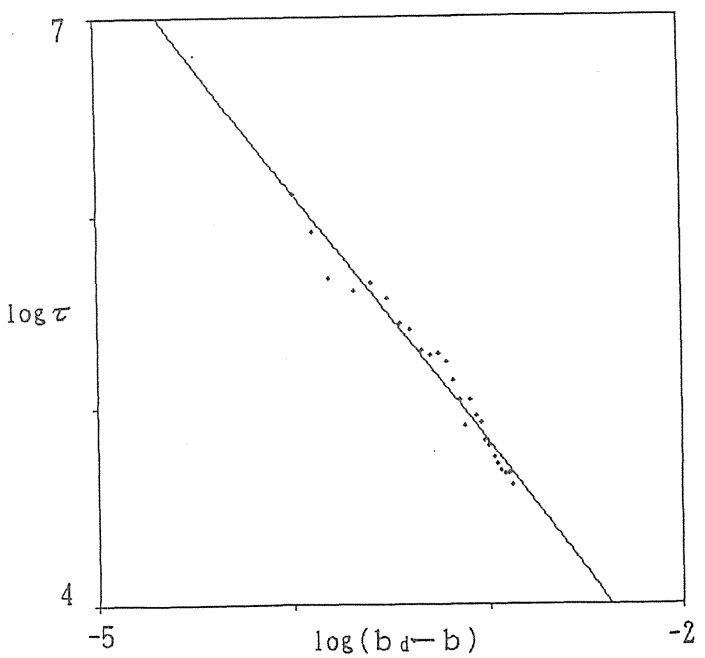

Fig.12

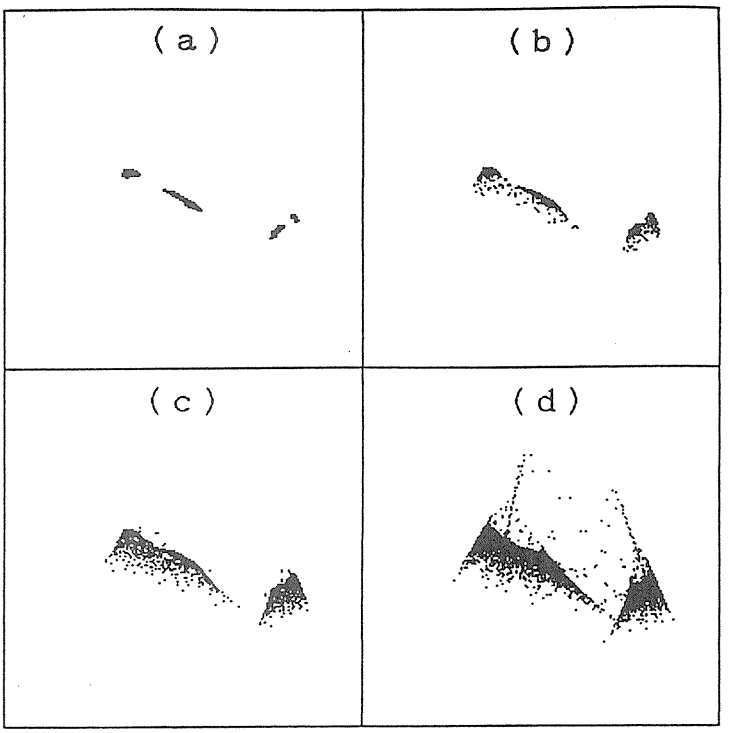

Fig.13

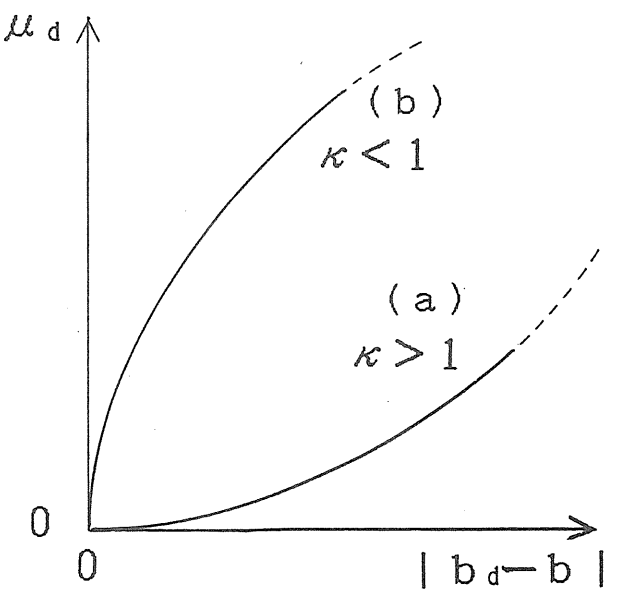

Fig.14